Journal of Fluorescence (2019) 29:1359–1369
https://doi.org/10.1007/s10895-019-02437-6

ORIGINAL ARTICLE

Synthesis of Strongly Fluorescent Imidazole Derivatives: Structure Property Studies, Halochromism and Fluorescent Photoswitching

Anu Kundu[1] · Subramanian Karthikeyan[2] · Dohyun Moon[3] · Savarimuthu Philip Anthony[1]

Received: 2 April 2019 / Accepted: 10 September 2019 / Published online: 14 November 2019

Abstract

New series of methoxy and hydroxyl group substituted triphenylamine (TPA)-imidazole fluorescent molecules (5-(diphenylamino)-2-(1H-phenanthro[9,10-d]imidazol-2-yl)phenol (1), 5-(diphenylamino)-2-(1-phenyl-1H-phenanthro[9,10-d]imidazol-2-yl)phenol (2), 5-(diphenylamino)-2-(4,5-diphenyl-1H-imidazol-2-yl)phenol (3), 5-(diphenylamino)-2-(1,4,5-triphenyl-1H-imidazol-2-yl)phenol (4), N-(3-methoxy-4-(1H-phenanthro[9,10-d]imidazol-2-yl)phenyl)-N-phenylbenzenamine (5), N-(3-methoxy-4-(1-phenyl-1H-phenanthro[9,10-d]imidazol-2-yl)phenyl)-N-phenylbenzene amine (6), and N-(3-methoxy-4-(4,5-diphenyl-1H-imidazol-2-yl)phenyl)-N-phenylbenzenamine (7)) have been synthesized that exhibited strong solution fluorescence and molecular structure and conformation controlled fluorescence photoswitching, solid state fluorescence and halochromism. Hydroxyl substituted molecules (1–4) showed moderate to strong fluorescence in solution depend on solvent polarity and very weak solid state fluorescence. Methoxy substituted molecules (5–7) displayed strong fluorescence both in solution and solid state. Solid state structural studies revealed strong intramolecular H-bonding in the crystal lattice. Interestingly, highly twisted structure (6) showed rare light induced reversible fluorescence switching in $CHCl_3$. The observation of isobestic point in time dependent fluorescence photoswitching studies indicated structural isomer conversion. Further, acid sensitive imidazole nitrogen has been made use to demonstrate solid state fluorescence switching via halochromism. Thus the present studies attempted to develop new fluorescent molecules and establish structure-property relationship for designing fluorescence switching materials.

Keywords Fluorescence switching · Halochromism · Fluorescence photoswitching · Solid state fluorescence

Highlights
- Fluorescent imidazole derivatives.
- Unusual reversible fluorescence switching.
- Substituent group dependent reversible solid state halochromism
- Molecular structure dependent solid state fluorescence.

Electronic supplementary material The online version of this article (https://doi.org/10.1007/s10895-019-02437-6) contains supplementary material, which is available to authorized users.

✉ Dohyun Moon
dmoon@postech.ac.kr

✉ Savarimuthu Philip Anthony
philip@biotech.sastra.edu

[1] School of Chemical & Biotechnology, SASTRA Deemed University, Thanjavur, Tamil Nadu 613401, India

[2] PG and Research department of chemistry, KhadirMohideen College, Adirampattinam, Tamil Nadu, India

[3] Beamline Department, Pohang Accelerator Laboratory, 80 Jigokro-127beongil, Nam-gu, Pohang, Gyeongbuk, South Korea

Introduction

Organic fluorescent molecules and materials that exhibited external stimuli induced fluorescence switching have been of great current interest because of their potential applications in security systems, displays, sensors, memory devices, data storage and optoelectronic devices including organic light emitting diodes (OLED) [1–17]. Triphenylamine (TPA), a propeller shaped optoelectronic molecule, has been extensively used as core for constructing strongly fluorescent materials for fabricating OLED device [18–23]. The conformational flexibility and synthetic advantage of TPA provided opportunity to realize aggregation enhanced emissive (AEE), stimuli-responsive smart fluorescent materials and tunable fluorescence via polymorphism [24–34]. TPA donor with quinoxaline-6,7-dicarbonitrile acceptor produced deep red to near infrared thermally activated delayed fluorescence in thin films as well as electroluminescent devices [35]. Host-guest complex formation and nanofabrication of TPA derivatives lead to tunable solid

state fluorescence [36–38]. TPA based acrylonitrile exhibited highly efficient fluorescent E and Z isomers with stable configurations under photo irradiation [39]. β-Iminoenolate boron complex with terminal TPA exhibited polymorphism induced fluorescence tuning and mechanofluorochromism [40]. High contrast mechanofluorochromism and bicolour electroluminescence has been demonstrated using a novel AEE active TPA derivative [41]. Multi-stimuli responsive, rewritable and self-erasable fluorescent platform has been achieved by incorporating pH responsive isoquinoline unit with TPA [42]. Molecular engineering of TPA derivatives with substituents and acceptor groups lead to topochemical conversion, defection and polymorphism induced fluorescence tuning and switching [43, 44]. Alkoxy carbon chain and position controlled rare positive enhancement of fluorescence with temperature, crystallization induced fluorescence switching in super cooled fluorescent liquid and molecular packing dependent fluorescence tuning has also been demonstrated [45–47]. TPA-Schiff base derivatives exhibited excited state intramolecular proton transfer (ESIPT) induced fluorescence and molecular conformation controlled mechanofluorochromism [48, 49].

Imidazole derivatives often exhibited strong fluorescence and enhanced thermal properties that made them as potential materials for optoelectronic devices [50–53]. Benzimidazole substituted radical derivatives showed efficient red-orange electroluminescence [54, 55]. ESIPT phenomena in imidazole derivatives exploited for fluorescence switching and tuning [56–59]. TPA attached imidazole derivatives showed improved electroluminescent properties [60, 61]. Hence we envisage that integrating acid responsive imidazole with mechanochromic TPA might produce multi-stimuli responsive smart fluorescent materials. In this manuscript, we report the synthesis of hydroxyl/methoxy substituted TPA-imidazole derivatives (Scheme 1) and investigation of fluorescence switching in solution as well as solid state. Hydroxyl substituted compounds showed weak fluorescence in solid state and strong to moderate fluorescence in solution depend on the polarity. Methoxy substituted compounds exhibited strong fluorescence in all solvents as well as solid state. Interestingly, compound 6 exhibited rare light induced fluorescence photoswitching in $CHCl_3$ and halochromism in solid state. Solid state structural and computational studies were performed to get insight on the fluorescence properties.

Experimental Sections

Materials

Triphenylamine, N-(3-methoxyphenyl)-N-phenylbenzenamine, dimethylformamide (DMF, HPLC grade), $POCl_3$, benzil, 9, 10-phenanthrenequinone were purchased from Sigma-Aldrich

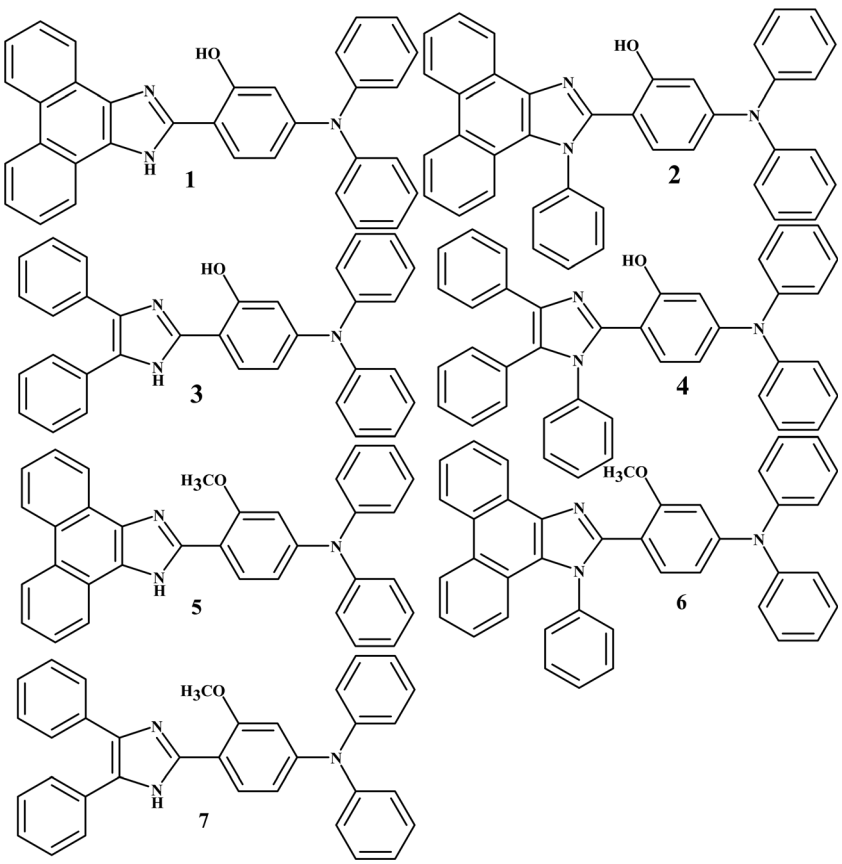

Scheme 1 Molecular structure of TPA-imidazole derivatives

and used without further purification. Ammonium acetate, glacial acetic acid, aniline and solvents were obtained from Merck India. 4-(diphenylamino) benzaldehyde, 4-(dipheny-lamino)-2-methoxybenzaldehyde and 4-(diphenylamino)-2-hydroxybenzaldehyde was synthesized following reported procedure [62, 63].NMR spectra were measured on a Bruker 300 MHz AVANCE-II. Absorption spectra were measured using Perking Elmer 1050. Fluorescence spectra and absolute quantum yield for all compounds in the solid state were recorded using Jasco fluorescence spectrometer-FP-8300 instruments equipped with integrating sphere and calibrated light source. Single crystals were coated with paratone-N oil and the diffraction data measured at 100 K with synchrotron radiation (λ = 0.62998 Å) on a ADSC Quantum-210 detector at 2D SMC with a silicon (111) double crystal monochromator (DCM) at the Pohang Accelerator Laboratory, Korea. CCDC Nos. – 1,865,289-1,865,294 contain the supplementary crystallographic data for this paper. The HOMO, LUMO and band gap of all structures are studied using B3PW91/6–31 + G(d,p) level theory (Gaussian 09 package). The calculations have been performed using TD-DFT-B3PW91 method with 6–31 + G(d,p) basis set using Gaussian 09 program package.

General Procedure (Scheme S1)

Aniline (1.0 mmol), aldehyde (1.0 mmol) and ammonium acetate (7.0 mmol) was added into glacial acetic acid (2 mL) at room temperature for 2, 4 and 6 whereas aldehyde (1.0 mmol) and ammonium acetate (7.0 mmol) was added into glacial acetic acid (2 mL) for 1, 3, 5 and 7. The resulting mixture was stirred for 4 h at 95 °C. The completion of the reaction was monitored by thin layer chromatography. After cooling, the reaction mixture was dumped into cold water. The resulting precipitate was filtered, washed with water and dried under vacuum. The white solid was purified with column chromatography.

5-(diphenylamino)-2-(1H-phenanthro[9,10-d]imidazol-2-yl)phenol (1): m.*p* = 139 °C. Yield = 65%. ^{1}H NMR (300 MHz, $CDCl_3$) δ 13.21 (bs, 1H), 10.13 (s, 1H), 8.71 (bs, 2H), 8.56 (d, *J* = 6.0 Hz, 1H), 8.04 (bs, 1H), 7.70–7.62 (m, 4H), 7.53 (d, *J* = 8.4 Hz, 1H), 7.31–7.26 (m, 4H), 7.18–7.15 (m, 4H), 7.11–7.06 (m, 2H), 6.77 (d, *J* = 2.1 Hz, 1H), 6.62 (dd, *J* = 8.4, 8.7 Hz, 1H). ^{13}C NMR (75 MHz, $CDCl_3$ + DMSO) δ 170.2, 158.4, 149.5, 149.1, 146.3, 128.9, 128.7, 127.3, 126.3, 125.6, 125.4, 124.7, 124.6, 123.1, 122.9, 121.5, 112.3, 109.2, 106.7. m/z calcd for $C_{33}H_{23}N_3O$ (M + H): 477.18, found: 477.17.

5-(diphenylamino)-2-(1-phenyl-1H-phenanthro[9,10-d]imidazol-2-yl)phenol (2): m.*p* = 192 °C. Yield = 48%. ^{1}H NMR (300 MHz, $CDCl_3$) δ 13.92 (bs, 1H), 8.76 (d, *J* = 8.7 Hz, 1H), 8.69 (t, *J* = 7.8 Hz, 2H), 7.78–7.62 (m, 7H), 7.50 (dt, *J* = 1.2, 7.6 Hz, 1H), 7.38–7.21 (m, 4H), 7.14–6.99 (m, 8H), 6.74 (d, *J* = 2.4 Hz, 1H), 6.51 (d, *J* = 9.0 Hz, 1H), 6.13 (dd, *J* = 9.0 Hz, 1H). ^{13}C NMR (75 MHz, $CDCl_3$) δ 160.5, 149.9, 148.9, 146.8, 139.2, 130.9, 130.6, 129.8, 129.4, 129.2, 129.2, 128.4, 127.4, 127.0, 126.6, 126.5, 126.4, 125.9, 125.7, 125.0, 124.2, 123.9, 123.2, 122.6, 120.7, 111.7, 109.8, 106.7. m/z calcd for $C_{39}H_{27}N_3O$ (M + H): 553.22, found: 553.20.

5-(diphenylamino)-2-(4,5-diphenyl-1H-imidazol-2-yl)phenol (3): m.*p* = 159 °C. Yield = 50%. ^{1}H NMR (300 MHz, $CDCl_3$) δ 9.16 (s, 1H), 7.61–7.55 (m, 4H), 7.35–7.25 (m, 11H), 7.16–7.14 (m, 4H), 7.09–7.05 (m, 2H), 6.72 (d, *J* = 2.1 Hz, 1H), 6.58 (dd, *J* = 8.4, 8.7 Hz, 1H). ^{13}C NMR (75 MHz, $CDCl_3$ + DMSO) δ 158.3, 149.2, 147.2, 146.5, 129.2, 128.4, 128.0, 127.3, 125.3, 125.0, 123.2, 113.5, 110.4, 107.7. m/z calcd for $C_{33}H_{25}N_3O$ (M + H): 479.20, found: 479.18.

5-(diphenylamino)-2-(1,4,5-triphenyl-1H-imidazol-2-yl)phenol (4): m.*p* = 165 °C. Yield = 70%. ^{1}H NMR (300 MHz, $CDCl_3$) δ 13.60 (bs, 1H), 7.54–7.51 (m, 2H), 7.35–7.33 (m, 3H), 7.27–7.19 (m, 12H), 7.14–7.11 (m, 6H), 7.08–7.03 (m, 2H), 6.71 (d, *J* = 2.1 Hz, 1H), 6.33 (d, *J* = 9 Hz, 1H), 6.10 (dd, *J* = 8.7 Hz, 1H),. ^{13}C NMR (75 MHz, $CDCl_3$) δ 159.6, 149.2, 147.2, 147.0, 145.3, 137.3, 134.8, 133.2, 131.4, 129.9, 129.9, 129.6, 129.4, 129.3, 129.1, 128.8, 128.4, 128.3, 128.3, 126.9, 126.3, 125.5, 125.3, 123.6, 111.9, 110.0, 106.9. m/zcalcd for $C_{39}H_{29}N_3O$ (M + H): 555.23, found: 555.4.

N-(3-methoxy-4-(1H-phenanthro[9,10-d]imidazol-2-yl)phenyl)-N-phenylbenzenamine (5): m.*p* = 232 °C. Yield = 88%. ^{1}H NMR (300 MHz, $CDCl_3$) δ 11.09 (s, 1H), 8.72 (d, *J* = 8.4 Hz, 3H), 8.53 (d, *J* = 8.4 Hz, 1H), 8.05 (bs, 1H), 7.70–7.58 (m, 4H), 7.35–7.29 (m, 4H), 7.20–7.17 (m, 4H), 7.11 (t, *J* = 7.3 Hz, 2H), 6.84 (d, *J* = 7.8 Hz, 1H), 6.74 (d, *J* = 1.8 Hz, 1H), 3.95 (s, 3H). ^{13}C NMR (75 MHz, $CDCl_3$) δ 157.1, 150.1, 147.6, 147.1, 130.2, 129.5, 128.2, 126.8, 125.2, 125.0, 123.8, 115.9, 105.2, 56.05. m/zcalcd for $C_{34}H_{25}N_3O$ (M + H): 491.20, found: 491.3.

N-(3-methoxy-4-(1-phenyl-1H-phenanthro[9,10-d]imidazol-2-yl)phenyl)-N-phenylbenzene amine (6): m.*p* = 223 °C. Yield = 90%. ^{1}H NMR (300 MHz, $CDCl_3$) δ 8.86 (dd, *J* = 8.1 Hz, 1H), 8.77 (d, *J* = 8.4 Hz, 1H), 8.70 (d, *J* = 8.4 Hz, 1H), 7.73–7.60 (m, 3H), 7.53–7.41 (m, 6H), 7.37–7.29 (m, 3H), 7.24–7.18 (m, 3H), 7.05 (d, *J* = 8.4 Hz, 6H), 6.62 (dd, *J* = 8.1 Hz, 1H),6.42 (d, *J* = 1.8 Hz, 1H). ^{13}C NMR (75 MHz, $CDCl_3$) δ 158.3, 150.6, 150.1, 147.3, 138.5, 137.4, 132.9, 129.5, 129.3, 129.1, 128.9, 128.7, 128.1, 127.4, 127.4, 127.2, 126.1, 125.3, 125.2, 124.8, 124.7, 124.1, 123.8, 123.4, 123.1, 122.8, 121.0, 115.0, 113.9, 105.4, 54.9. m/z calcd for $C_{40}H_{29}N_3O$ (M + H): 567.23, found: 567.4.

N-(3-methoxy-4-(4,5-diphenyl-1H-imidazol-2-yl)phenyl)-N-phenylbenzenamine (7): m.*p* = 238 °C. Yield = 90%. ^{1}H NMR (300 MHz, $CDCl_3$) δ 7.59 (dd, *J* = 8.4, 7.8 Hz, 2H), 7.46 (d, *J* = 8.1 Hz, 1H), 7.27–7.20 (m, 6H), 7.18–7.13 (m, 6H), 7.08–7.00 (m, 6H), 6.95–6.92 (m, 2H), 6.65 (dd, *J* = 8.4 Hz, 1H), 6.36 (d, *J* = 2.1 Hz, 1H), 3.11 (s, 3H). ^{13}C

NMR (75 MHz, $CDCl_3$) δ 157.7, 156.5, 150.3, 147.5, 147.3, 145.5, 137.9, 137.4, 132.8, 131.1, 131.1, 130.9, 130.5, 129.6, 129.4, 129.3, 129.2, 129.0, 128.5, 128.4, 128.3, 128.2, 128.1, 128.0, 127.9, 127.8, 127.7, 127.6, 127.4, 127.3, 126.5, 125.3, 125.1, 124.8, 123.9, 123.3, 120.8, 115.3, 114.8, 105.5, 54.6. m/z calcd for $C_{40}H_{29}N_3O$ (M + H): 493.22, found: 493.3.

Results and Discussion

Methoxy/hydroxyl substituted TPA donor attached imidazole accepter that consist of flexible/rigid aromatic unit has been synthesized by following the reported literature (Scheme 1, S1, 64]. Absorption studies of 1–7 did not show significant variation in the absorption λ_{max} across solvent polarity (Fig. 1, S1, 2, Table S1). This indicates that the ground state of the molecules is not considerably polar to be influenced by solvent polarity. All molecules exhibited strong n-π* transition compared to π-π* transition. 1 showed absorption between 366 and 389 nm depend on the solvent polarity. 2 and 3 showed absorption between 369 and 390 nm and 357 and 364 nm, respectively. Similarly, 4–7 also exhibited only slight variation in the absorption peak in different solvent polarity. Rigid phenanthrene incorporated molecules (1, 2 and 5) showed vibronic splitting in the absorption spectra. Methoxy substituted molecules showed relatively blue shifted absorption compared to hydroxyl substituted compounds that could be attributed to the molecular conformation and inter/intramolecular H-bonding. 6 showed strongest blue shift of absorption that can have strong twisting in the molecular structure due to methoxy and aniline attachment in the structure. Single crystal structure that will be discussed later part also confirmed high twisting of molecular structure. The fluorescence spectra of 1–7 also did not show significant change in the peaks position in different solvent polarity (Fig. 2, S3–4, Table S2). This suggests that excited state of the molecules also not significantly polar to be influenced by solvent polarity. For instance, the fluorescence λ_{max} was observed between 415 and 437 nm for 1 whereas 420 to 435 nm was observed for 2. Methoxy substituted 5 showed fluorescence λ_{max} between 413 and 421 nm. Other compounds also showed similar slight variation of λ_{max}. Quantum yield (Φ_f) measurements of 1–7 indicated strong fluorescence in the solution state

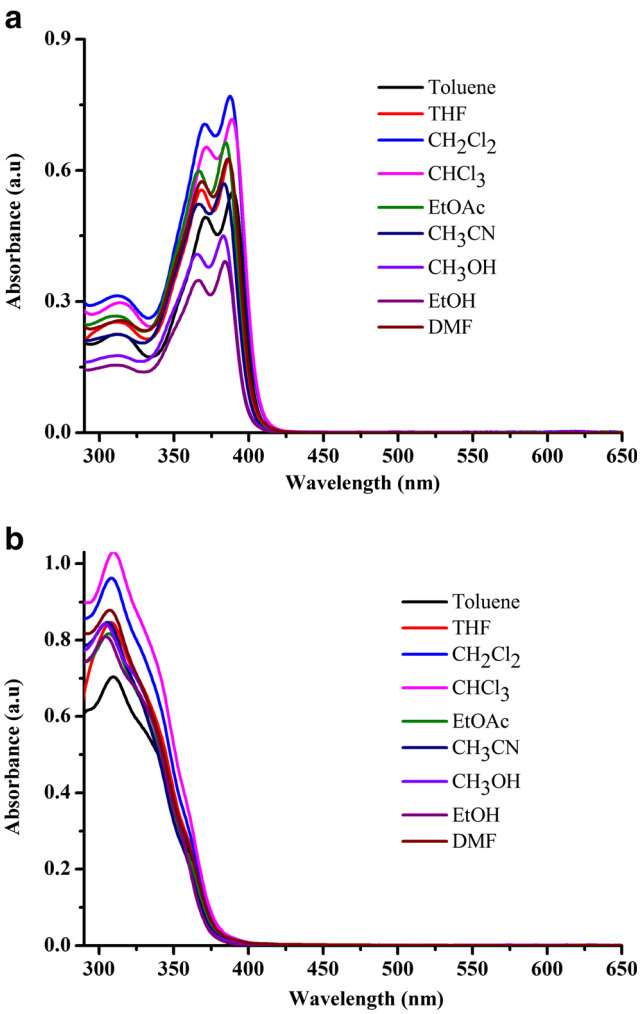

Fig. 1 Absorption spectra of 1 and 6 in different solvents

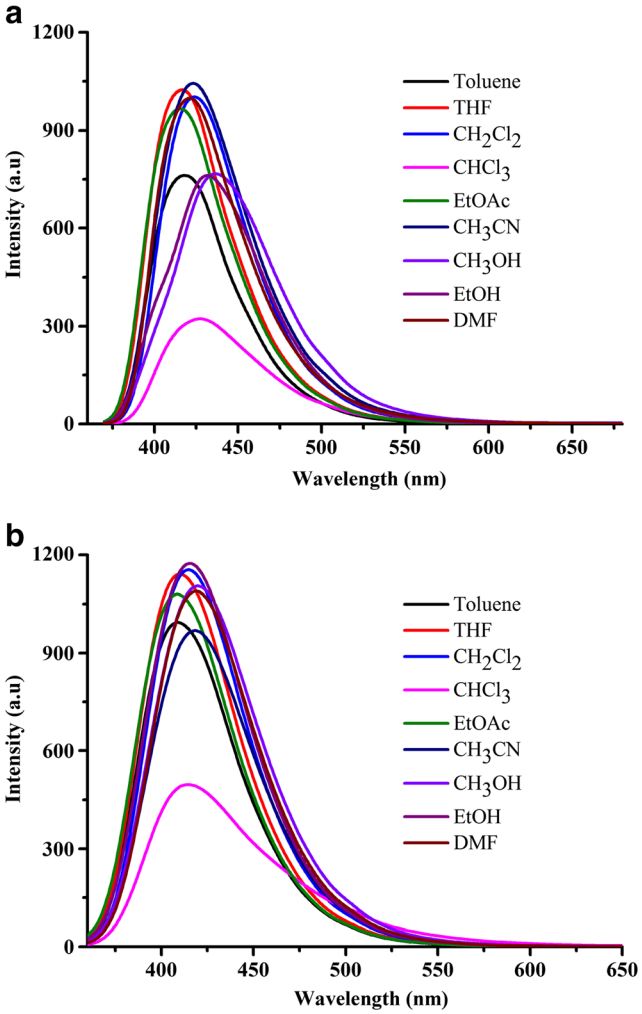

Fig. 2 Fluorescence spectra of 1 and 6 in different solvents (10^{-5} M)

(Table S3). Hydroxyl substituted 1–4 exhibited relatively strong fluorescence in non-polar solvents compared to polar solvents that could be attributed to the intermolecular interactions between the polar solvents with labile hydroxyl proton. In contrast, methoxy substituted 5–7 displayed strong fluorescence in polar to non-polar solvents since there is no strong interacting functionality present in the structure.

Interestingly, methoxy substituted compounds particularly 5 and 6 showed light induced fluorescence photoswitching in $CHCl_3$. Absorption spectra of 5 showed two clear peaks at 370 and 386 nm before UV exposure. After UV light exposure (365 nm), single peak was observed at 390 nm along with a small hump at 485 nm (Fig. S5a). The small hump was disappeared after 24 h and peak at 390 nm has also been blue shifted to 386 nm with appearance weak hump at 370 nm (Fig. S6). 5 showed fluorescence at 420 nm in $CHCl_3$ before light irradiation. After light irradiation, fluorescence peak was red shifted to 464 nm (Fig. 3a). Time dependent kinetic studies showed drastic reduction of fluorescence intensity at 420 nm and appearance of fluorescence at 474 nm within five minutes (Fig. 4a, S7a). Only a slight hump was observed at 420 nm after UV irradiation. The fluorescence modulation was completed within 40 min. Further irradiation did not show significant change of fluorescence intensity or λ_{max}. The red shifted fluorescence was stable for long time (24 h) in presence of white light. After 24 h it showed decrease of fluorescence intensity with blue shift of peak position as well as appearance of hump at 420 nm (Fig. S8). However, the fluorescence did not clearly return to the initial state even after 72 h. It is noted that 5 in CH_2Cl_2 also exhibited decrease of intensity with slight red shift of peak position (430 nm). In contrast, the molecule showed good photo-stability in CH_3CN, EtOAc and THF (Fig. S9). 6 exhibited absorption at 309 nm before irradiation and showed new peak at 350 nm with reduction of intensity at 309 nm after irradiation (Fig. S5b). The new peak was completely disappeared after 24 h (Fig. S10). Similarly, fluorescence peak of 6 in $CHCl_3$ exhibited clear tuning from 415 to 472 nm by UV irradiation (Fig. 3b). Time dependent studies revealed gradual decrease of fluorescence intensity at 415 nm and appearance of new peak at 465 nm (Fig. 4b). The

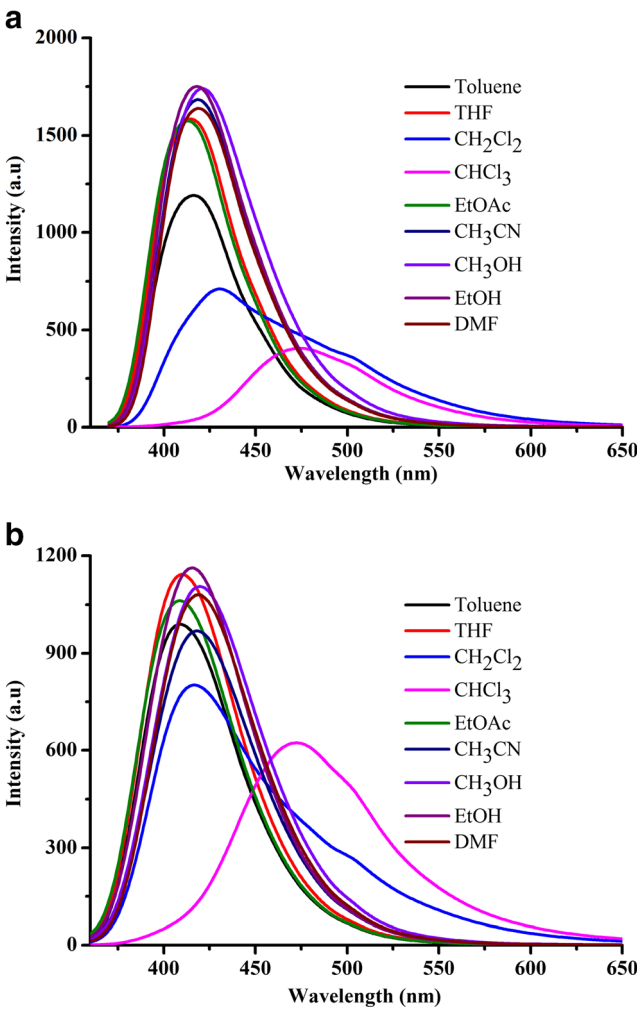

Fig. 3 Fluorescence spectra of (**a**) 5 and (**b**) 6 in $CHCl_3$ (10^{-5} M) after UV irradiation (λ_{exc} = 365 nm)

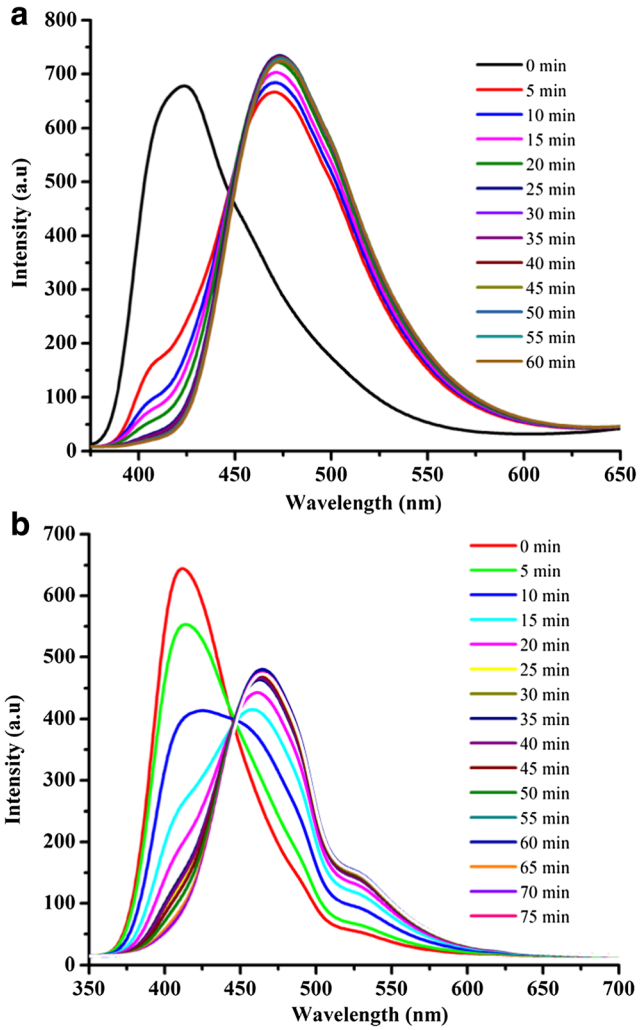

Fig. 4 Time dependent fluorescence spectra of (**a**) 5 and (**b**) 6 in $CHCl_3$(10^{-5} M) under UV irradiation (λ_{exc} = 365 nm)

Scheme 2 Schematic representation of light Conformational modulation of 6

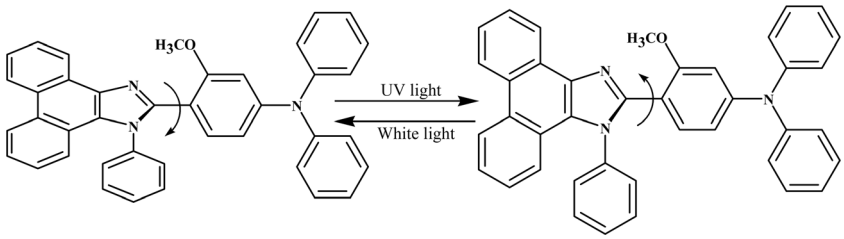

tuning of fluorescence has been completed within 60 min (Fig. S7b). The appearance of clear isobestic point at 444 nm indicates the interconversion from twisted conformational isomer to planar isomer in $CHCl_3$ by light irradiation. The reverse studies showed slow decrease of fluorescence intensity with appearance of peak at 415 nm. The complete fluorescence switching has taken much longer time (18 h) compared to forward fluorescence tuning (Fig. S11). However, unlike 5, the fluorescence of 6 has been completely switched to initial state. It is noted that 5 and 6 kept at dark after irradiation did not show significant fluorescence switching and only in presence of white light fluorescence switching was observed. The isobestic point was appeared at same wavelength in reverse process also. Photo-stability studies showed good stability for 6 also in CH_3CN, EtOAc and THF under UV light (Fig. S12). Hydroxyl group substituted 1–4 exhibited strong reduction of fluorescence intensity under UV light exposure that could be due to labile hydroxyl group. Similarly 7 also did not show significant modulation of fluorescence after UV irradiation. Molecular structure of 6 can exhibit twisted conformation between imidazole unit and TPA phenyl group. The twisted molecular structure of 6 has also been confirmed by single crystal structural analysis (discussed latter part). Hence the twisted molecular conformation of 6 might produce more planar conformation upon UV irradiation (Scheme 2). NMR studies of 5 and 6 before and after UV irradiation did not show any significant change in the peak position and suggest that there may not be any structural modification chemically by light irradiation (Fig. S13 and S14). It is noted that organic molecules mostly exhibited fluorescence photoswitching either via ring opening/closing or E/Z isomerization [65, 66]. Even ring opening/closing or E/Z isomerization often exhibited on-off or off-on fluorescence switching rather between two fluorescence states.

To get the insight on the molecular conformation, single crystal structural analysis has been performed for 1–7 except 3. Attempted crystallization of 3 from different solvents did not produce quality single crystals for structural studies. Molecular structure with aniline attachment at one of the imidazole nitrogen (2, 4 and 6) resulted in twisted molecular conformation between TPA phenyl and imidazole unit whereas without aniline substitution (1, 5 and 7) displayed coplanar conformation (Fig. 5). Molecular twist between imidazole unit and TPA phenyl group can be expressed using torsion angle

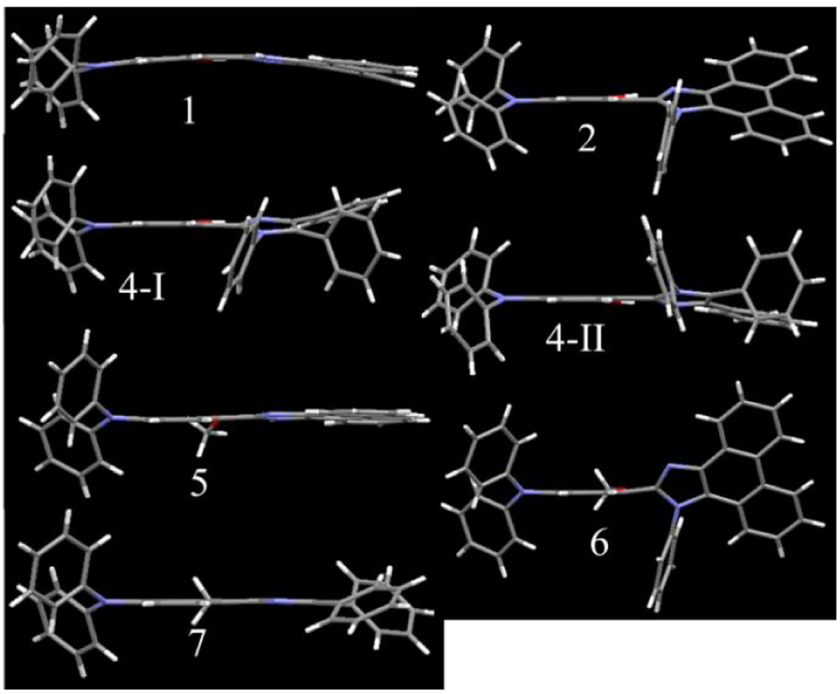

Fig. 5 Molecular conformation of 1–7 in the crystal lattice. C (grey), N (blue), O (red), H (white)

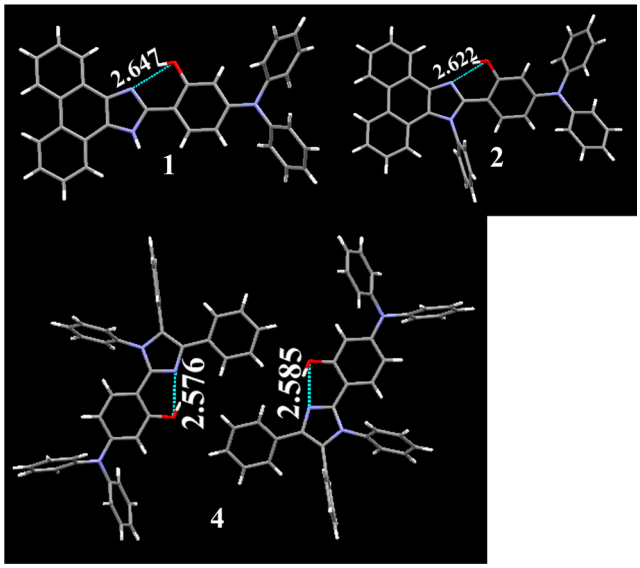

Fig. 6 Intramolecular interactions in the crystal lattice of 1, 2 and 4. C (grey), N (blue), O (red), H (white); H-bonds (broken line). $d_{D\ldots A}$ distances are marked (Å)

(τ) that showed higher angle for 2, 4 and 6 compared to 1, 5 and 7 (Table S4). Hydroxyl group substituted 1, 2 and 4 exhibited strong intramolecular H-bonding between hydroxyl oxygen and imidazole nitrogen atom (Fig. 6). Solvent molecule has been included in the crystal lattice of 1 and 6 that was stabilized by H-bonding interaction between carbonyl oxygen and imidazole nitrogen (Fig. S15). Further, solvent molecule in the crystal lattice of 6 exhibited disordered structure. All molecules showed dimer formation with opposite molecular arrangement except 6 in the crystal lattice via weak intermolecular interactions (Fig. 7). 1 showed perfect opposite molecular arrangement via C-H…π interaction between TPA phenyl hydrogen and phenanthrene ring. H-bonding interaction between methoxy oxygen and phenanthrene hydrogen produced slipped dimer formation in the crystal lattice of 2. 4 showed dimer via π…π interactions between imidazole phenyl groups. 5 and 7 exhibited dimer via C-H…π and C-H…N intermolecular interactions. In contrast, 6 exhibited parallel arrangement molecules through C-H…π and C-H…N intermolecular interactions and next layer along *a*-axis adopted opposite arrangement molecules but without any intermolecular interactions (Fig. S16). Thus single crystal structure clearly indicated that 6 exhibited highest molecular twist between TPA phenyl and imidazole unit compared to other compounds. We speculate that upon light irradiation might convert the twisted structure to more planar structure that lead to red shift of absorption and fluorescence (Scheme 2). Although 2 and 4 exhibited considerable molecular twist, the labile hydroxyl group might be contributing for reduction of fluorescence upon light irradiation.

The incorporation of propeller shaped TPA unit along with imidazole unit resulted in solid state fluorescence in all seven compounds (Fig. 8). 1 and 2 showed fluorescence λ_{max} at 444 nm whereas 3 and 4 exhibited fluorescence at 434 and 422 nm, respectively. 5 showed largest red shifted fluorescence at 452 nm and 7 displayed highest blue shifted fluorescence at 393 nm with small Stokes shift (18 nm). 6 that exhibited highest molecular twist showed fluorescence at 427 nm. Absolute quantum (Φ_f) yield measurement revealed weak fluorescence for hydroxyl substituted compounds (0.96% (1), 2.89% (2), 0.57% (3) and 1.69% (4)) and strong fluorescence for methoxy substituted compounds (7.59% (5), 13.81% (6) and 19.60% (7)). The presence of hydroxyl group in 1–4 and strong

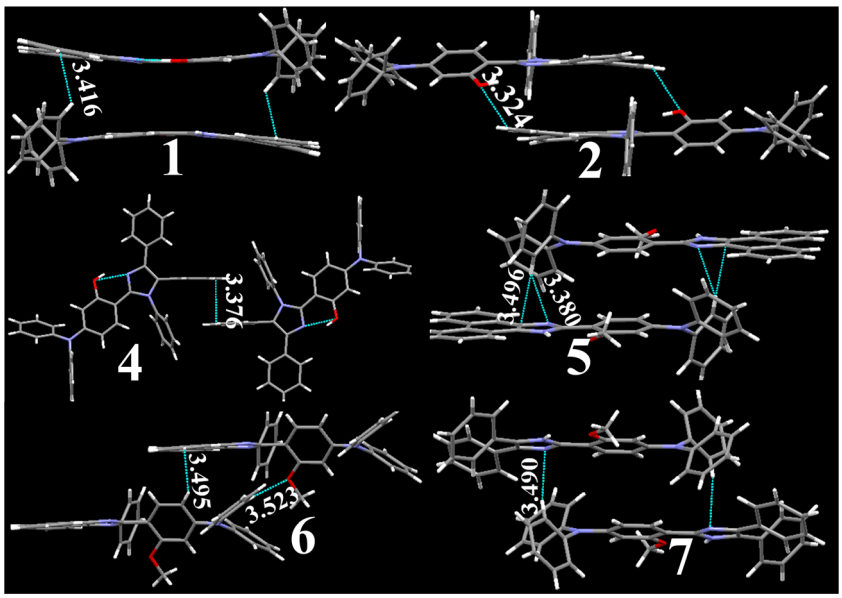

Fig. 7 Molecular dimer formation in the crystal lattice of 1-2 and 4-7. C (grey), N (blue), O (red), H (white); H-bonds (broken line). $d_{D\ldots A}$ distances are marked (Å)

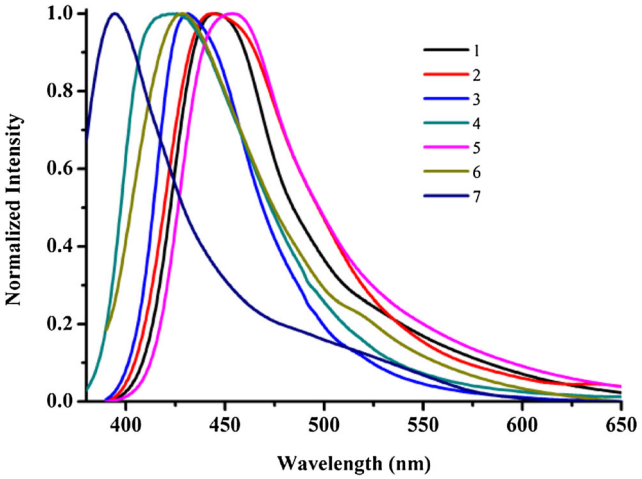

Fig. 8 Solid state fluorescence of 1–7 (λ_{exc} = 360 nm)

intramolecular H-bonding that was evidenced from the single crystal structure is expected to exhibit excited state intramolecular proton transfer (ESIPT) process induced fluorescence [56–59]. However, weak solid state fluorescence and small Stoke shift (69 to 47 nm) indicates that the compounds did not show ESIPT induced fluorescence since ESIPT process expected to display large Stoke shift with enhanced fluorescence. Similarly, the molecule with highest twist might often show strong blue shifted fluorescence due to hindering electronic conjugation. In contrast, less twisted coplanar 7 showed strongly blue shifted emission with highest intensity. Highest twisted structure of 6 exhibited relatively low intensity but red shifted fluorescence compared to 7. 5 with slightly twisted molecular structure exhibited large red shift and weak fluorescence compared to 6 and 7. These results suggest that solid state fluorescence properties are not only controlled by molecular conformation of individual molecule and also by how adjacent molecules are organized and interact with each other in the crystal lattice. Molecular packing of 7 revealed alternate arrangement of dimer with opposite molecular arrangement along *bc*-plane (Fig. S16c). In 6, adjacent layer adopted opposite arrangement along *a*-axis whereas dimers are well separated in the crystal lattice of 5 (Fig. S16a,b). Hence, although molecular structure of 6 exhibited highest twist its opposite arrangement of dipoles in adjacent layers compared to adjacent molecules in 7 resulted in slightly red shifted fluorescence. HOMO-LUMO calculations of 5–7 revealed molecular twist controlled optical band gap (Table 1). Highly twisted structure exhibited highest band gap compared to more planar structure. Solid state

Table 1 Optical band gap of 5–7

	HOMO (eV)	LUMO (eV)	Band gap (eV)
5	−5.043	−1.279	3.76
6	−5.149	−1.150	4.00
7	−4.945	−1.034	3.91

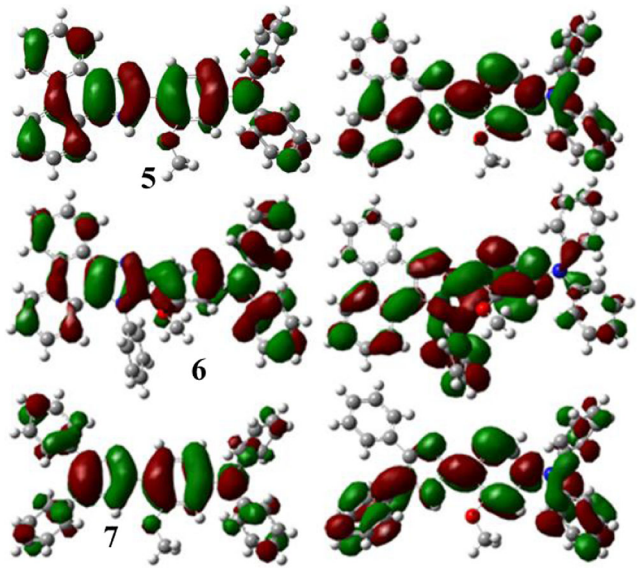

Fig. 9 HOMO-LUMOs of 5–7

fluorescence of planar 5 showed red shifted emission whereas twisted structure of 6 lead to blue shifted fluorescence. In contrast, 7 that exhibited strong blue shift of fluorescence revealed optical band gap slightly lower than 6. This might be attributed to the long tail observed in the fluorescence spectrum of 6 (Fig. 8). The electron density of 5 showed more spread occupancy in complete structure both in HOMO and LUMO that supported the red shifted fluorescence (Fig. 9). In contrast, twisted structure of 6 showed clear electron transfer from TPA diphenyl ring and phenanthrene in HOMO to TPA phenyl ring attached to imidazole unit in LUMO. Similarly, 7 showed electron transfer from benzil phenyl in HOMO to TPA-imidazole unit in LUMO. Strong solid state fluorescence along with pH responsive imidazole nitrogen provided opportunity to explore halochromic fluorescence switching in 5–7. We have chosen 5–7 compounds to investigate halochromism due to strong fluorescence as well as absence of hydroxyl group that might interfere in acid-base exposure. Trifluoroacetic acid (TFA)

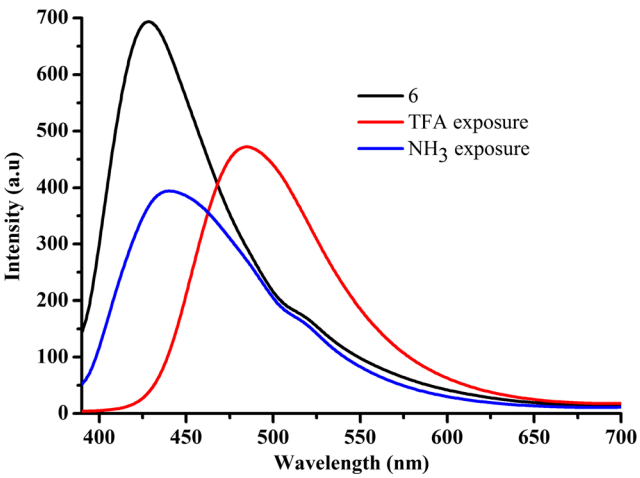

Fig. 10 Halochromism of 6

exposure onto 5 leads to fluorescence tuning from 452 to 502 nm (Fig. S17). NH_3 exposure blue shifted the fluorescence but only up to 480 nm. The fluorescence of 6 has also been red shifted from 427 to 490 nm upon exposure of TFA and NH_3 exposure completely reversed fluorescence to initial state (Fig. 10). In contrast, 7 did not show clear shift in the fluorescence upon exposure of TFA rather it exhibited substantial reduction of fluorescence intensity. The presence of unprotected imidazole amine nitrogen in 5 might have formed strong H-bonding interaction with TFA that might inhibit complete reversal of fluorescence upon NH_3 exposure. Hence, aniline attached highly twisted 6 exhibited reversible fluorescence switching between 427 and 490 upon TFA exposure and NH_3.

Conclusion

In conclusion, methoxy and hydroxyl group substituted TPA-imidazole fluorescence molecules have been synthesized and demonstrated molecular structure dependent fluorescence photoswitching and halochromism. Interestingly, 6 with strong twisted molecular structure showed rare light induced reversible fluorescence switching in $CHCl_3$. Time dependent fluorescent photoswitching studies indicated structural conversion from highly twisted isomer to planar isomer in $CHCl_3$ upon UV light exposure and white light exposure convert planar to twisted structure. The structure-property studies suggest that free amino nitrogen in the imidazole ring and labile hydroxyl group might not be good for fluorescence photoswitching. Also absence of hydroxyl and free imidazole amine nitrogen was important for solid state fluorescence switching via halochromism. Further, this study indicated that although molecular structure favored intramolecular H-bonding it need not exhibit ESIPT induced solid state fluorescence. Overall, the present studies resulted in finding rare phenomenon of molecular conformation controlled fluorescence photoswitching in imidazole derivatives.

Acknowledgments Financial support from the Science and Engineering Research Board (SERB), New Delhi, India (SERB No. EMR/2015/001891) is acknowledged with gratitude. "X-ray crystallography at the PLS-II 2D-SMC beamline was supported in part by MSIP and POSTECH.

References

1. Chi Z, Zhang X, Xu B, Zhou X, Ma C, Zhang Y, Liu S, Xu J (2012) Recent advances in organic mechanofluorochromic materials. Chem Soc Rev 41:3878–3896
2. Sagara Y, Kato T (2009) Mechanically induced luminescence changes in molecular assemblies. Nat Chem 1:605–610
3. Sagara Y, Yamane S, Mitani M, Weder C, Kato T (2016) Mechanoresponsive luminescent molecular assemblies: an emerging class of materials. Adv Mater 28:1073–1095
4. Ito H, Saito T, Oshima N, Kitamura N, Ishizaka S, Hinatsu Y, Wakeshima M, Kato M, Tsuge K, Sawamura M (2008) Reversible Mechanochromic luminescence of [(C6F5Au)2(μ-1,4-Diisocyanobenzene)]. J Am Chem Soc 130:10044–10045
5. (2014) Mechanochromic Fluorescent Materials: Phenomena, Materials and Applications, ed. Xu J, Chi Z, vol. 8, RSC, Cambridge
6. Weder C (2011) Mechanoresponsive materials. J Mater Chem 21: 8235–8236
7. Ciardelli F, Ruggeri G, Pucci A (2013) Dye-containing polymers: methods for preparation of mechanochromic materials. Chem Soc Rev 42:857–870
8. Saragi TPI, Spehr T, Siebert A, Fuhrmann-Liekerand T, Salbeck J (2007) Spiro compounds for organic optoelectronics. Chem Rev 107:1011–1065
9. Liang J, Tang BZ, Liu B (2015) Specific light-up bioprobes based on AIEgen conjugates. Chem Soc Rev 44:2798–2811
10. Yuan L, Lin WY, Zheng KB, He WL, Huang MW (2013) Far-red to near infrared analyte-responsive fluorescent probes based on organic fluorophore platforms for fluorescence imaging. Chem Soc Rev 42:622–661
11. Zhu YX, Wei ZW, Pan M, Wang HP, Zhang JY, Su CY (2016) A new TPE-based tetrapodal ligand and its ln(III) complexes: multi-stimuli responsive AIE (aggregation-induced emission)/ILCT(intra ligand charge transfer)-bifunctional photoluminescence and NIR emission sensitization. Dalton Trans 45:943–950
12. Zheng R, Mei XF, Lin ZH, Zhao Y, Yao HM, Lv W, Ling QD (2015) Strong CIE activity, multi-stimuli-responsive fluorescence and data storage application of new diphenyl maleimide derivatives. J Mater Chem C 3:10242–10248
13. Xu B, Xie M, He J, Xu B, Chi Z, Tian W, Jiang L, Zhao F, Liu S, Zhang Y, Xu Z, Xu J (2013) An aggregation-induced emission luminophore with multi-stimuli single- and two-photon fluorescence switching and large two-photon absorption cross section. Chem Commun 49:273–275
14. Kishimura A, Yamashita T, Yamaguchi K, Aida T (2005) Rewritable phosphorescent paper by the control of competing kinetic and thermodynamic self-assembling events. Nat Mater 4: 546–549 40:2400–2408
15. Hirata S, Watanabe T (2006) Reversible Thermoresponsive recording of fluorescent images (TRF). Adv Mater 18:2725–2729
16. Kwon MS, Gierschner J, Yoon SJ, Park SY (2012) Unique Piezochromic fluorescence behavior of Dicyanodistyrylbenzene based donor–acceptor–donor triad: mechanically controlled photo-induced Electron transfer (eT) in molecular assemblies. Adv Mater 24:5487–5492
17. Sun H, Liu S, Lin W, Zhang KY, Lv W, Huang X, Huo F, Yang H, Jenkins G, Zhao Q, Huang W (2014) Smart responsive phosphorescent materials for data recording and security protection. Nat Commun 5:3601–3609
18. Lee H, Sohn J, Hwang J, Park SY (2004) Triphenylamine-cored bifunctional organic molecules for two-photon absorption and Photorefraction. Chem Mater 16:456–465
19. Sonntag M, Kreger K, Hanft D, Strohriegl P (2005) Novel star-shaped Triphenylamine-based molecular glasses and their use in OFETs. Chem Mater 17:3031–3039
20. Li H, Fang M, Tang R, Hou Y, Liao Q, Mei A, Han H, Li Q, Li Z (2016) The introduction of conjugated isolation groups into the common acceptor cyanoacrylic acid: an efficient strategy to suppress the charge recombination in dye sensitized solar cells and the dramatically improved efficiency from 5.89% to 9.44%. J Mater Chem A 4:16403–16409

21. Shih PI, Chien CH, Wu FI, Shu CF (2007) A novel Fluorene-Triphenylamine hybrid that is a highly efficient host material for blue-, green-, and red-light-emitting Electrophosphorescent devices. Adv Funct Mater 17:3514–3520
22. Kundu A, Karthikeyan S, Moon D, Anthony SP (2017) Self-reversible thermofluorochromism of D–A–D triphenylamine derivatives and the effect of molecular conformation and packing. CrystEngComm 19:6979–6985
23. Woo SJ, Kim Y, Kim MJ, Baek JY, Kwon SK, Kim YH, Kim JJ (2018) Strategies for the molecular Design of Donor–Acceptor-type Fluorescent Emitters for efficient deep blue organic light emitting diodes. Chem Mater 30:857–863
24. Ning ZJ, Chen Z, Zhang Q, Yan YL, Tian H (2007) Aggregation-induced emission (AIE)-active starburst Triarylamine fluorophores as potential non-doped red emitters for organic light-emitting diodes and Cl_2 gas Chemodosimeter. Adv Funct Mater 17:3799–3807
25. Chi ZG, Zhang XQ, Xu BJ, Zhou X, Ma CP, Zhang Y, Liu SW, Xu JR (2012) Recent advances in organic mechanofluorochromic materials. Chem Soc Rev 41:3878–3896
26. Ning Z, Tian H (2009) Triarylamine: a promising core unit for efficient photovoltaic materials. Chem Commun:5483–5495
27. Malagoli M, Bredas JL (2000) Density functional theory study of the geometric structure and energetics of triphenylamine-based hole-transporting molecules. Chem Phys Lett 327:13–17
28. Yuan WZ, Gong Y, Chen S, Shen XY, Lam JW, Lu P, Lu Y, Wang Z, Hu RR, Xie N, Kwok HS, Zhang YM, Sun JZ, Tang BZ (2012) Efficient solid emitters with aggregation-induced emission and intramolecular charge transfer characteristics: molecular design, synthesis, Photophysical behaviors, and OLED application. Chem Mater 24:1518–1528
29. Cao Y, Xi W, Wang L, Wang H, Kong L, Zhou H, Wu J, Tian Y (2014) Reversible piezofluorochromic nature and mechanism of aggregation-induced emission-active compounds based on simple modification. RSC Adv 4:24649
30. Fang M, Yang J, Liao Q, Gong Y, Xie Z, Chi Z, Peng Q, Li Q, Li Z (2017) Triphenylamine derivatives: different molecular packing and the corresponding mechanoluminescent or mechanochromism property. J Mater Chem C 5:9879–9885
31. Gong Y, Tan Y, Liu J, Lu P, Feng C, Yuan WZ, Lu Y, Sun JZ, He G, Zhang Y (2013) Twisted D–π–a solid emitters: efficient emission and high contrast mechanochromism. Chem Commun 49: 4009–4011
32. Gong Y, Liu J, Zhang Y, He G, Lu Y, Fan WB, Yuan WZ, Sun JZ, Zhang Y (2014) AIE-active, highly thermally and morphologically stable, mechanochromic and efficient solid emitters for low color temperature OLEDs. J Mater Chem C 2:7552–7560
33. Hariharan PS, Gayathri P, Kundu A, Karthikeyan S, Moon D, Anthony SP (2018) Synthesis of tunable, red fluorescent aggregation-enhanced emissive organic fluorophores: stimuli-responsive high contrast off–on fluorescence switching. CrystEngComm 20:643–651
34. Wang K, Zhang H, Chen S, Yang G, Zhang J, Tian W, Su Z, Wang Y (2014) Organic polymorphs: one-compound-based crystals with molecular- conformation- and packing-dependent luminescent properties. Adv Mater 26:6168–6173
35. Li C, Duan R, Liang B, Han G, Wang S, Ye K, Liu Y, Yi Y, Wang Y (2017) Deep-red to near-infrared thermally activated delayed fluorescence in organic solid films and electroluminescent devices. Angew Chem Int Ed 56:11525–11529
36. Gangopadhyay M, Mandal AK, Maity A, Ravindranathan S, Rajamohanan PR, Das A (2016) Tuning emission responses of a Triphenylamine derivative in host–guest complexes and an unusual dynamic inclusion phenomenon. J Organomet Chem 81:512–521
37. Anthony SP, Varughese S, Draper SM (2009) Switching and tuning organic solid-state luminescence via a supramolecular approach. Chem Commun:7500–7502
38. Anthony SP, Draper SM (2010) Nano/microstructure fabrication of functional organic material: polymorphic structure and tunable luminescence. J Phys Chem C 114:11708–11716
39. Li W, Wang S, Zhang Y, Gao Y, Dong Y, Zhang X, Song Q, Yang B, Ma Y, Zhang C (2017) Highly efficient luminescent E- and Z-isomers with stable configurations under photoirradiation induced by their charge transfer excited states. J Mater Chem C 5:8097–8104
40. Zhang Z, Wu Z, Sun J, Yao B, Xue P, Lu R (2016) β-Iminoenolate boron complex with terminal triphenylamine exhibiting polymorphism and Mechanofluorochromism. J Mater Chem C 4:2854–2861
41. Hu J, Jiang B, Gong Y, Liu Y, He G, Yuan WZ, Wei C (2018) A novel triphenylacrylonitrile based AIEgen for high contrast mechanchromism and bicolor electroluminescence. RSC Adv 8:710–716
42. Hariharan PS, Mothi EM, Moon D, Anthony SP (2016) Halochromic Isoquinoline with MechanochromicTriphenylamine: smart fluorescent material for rewritable and self-erasable fluorescent platform. ACS Appl Mater Interfaces 8:33034–33042
43. Hariharan PS, Moon D, Anthony SP (2015) Reversible fluorescence switching and topochemical conversion in an organic AEE material: polymorphism, defection and nanofabrication mediated fluorescence tuning. J Mater Chem C 3:8381–8388
44. Hariharan PS, Gayathri P, Kundu A, Karthikeyan S, Moon D, Sagara Y, Anthony SP (2018) Drastic modulation of stimuli-responsive fluorescence by a subtle structural change of organic fluorophore and polymorphism controlled Mechanofluorochromism. Cryst Growth Des 18:3971–3979
45. Hariharan PS, Mothi EM, Moon D, Anthony SP (2017) Crystallization-induced reversible fluorescence switching of alkyl chain length dependent thermally stable supercooled organic fluorescent liquids. CrystEngComm 19:6489–6497
46. Hariharan PS, Venkataramanan NS, Moon D, Anthony SP (2015) Self-reversible Mechanochromism and Thermochromism of a Triphenylamine-based molecule: tunable fluorescence and nanofabrication studies. J Phys Chem C 119:9460–9469
47. Hariharan PS, Gayathri P, Moon D, Anthony SP (2017) Tunable and switchable solid state fluorescence: alkyl chain length-dependent molecular conformation and self-reversible Thermochromism. ChemistrySelect 2:7799–7807
48. Kundu A, Karthikeyan S, Moon D, Anthony SP (2018) Molecular conformation- and packing-controlled excited state intramolecular proton transfer induced solid-state fluorescence and reversible Mechanofluorochromism. ChemistrySelect 3:7340–7345
49. Kundu A, Karthikeyan S, Moon D, Anthony SP (2018) Excited state intramolecular proton transfer induced fluorescence in triphenylamine molecule: role of structural conformation and reversible Mechanofluorochromism. J Mol Struct 1169:1–8
50. Ge Z, Hayakawa T, Ando S, Ueda M, Akiike T, Miyamoto H, Kajita T, Kakimoto M (2008) Spin-coated highly efficient phosphorescent organic light-emitting diodes based on bipolar Triphenylamine-Benzimidazole derivatives. Adv Funct Mater 18: 584–590
51. Zhuang S, Shangguan R, Jin J, Tu G, Wang L, Chen J, Ma D, Zhu X (2012) Efficient nondoped blue organic light-emitting diodes based on phenanthroimidazole-substituted anthracene derivatives. Org Electron 13:3050–3059
52. Kautny P, Wu Z, Eichelter J, Horkel E, Stöger B, Chen J, Ma D, Fröhlich J, Lumpi D (2016) Indolo[3,2,1-*jk*]carbazole based planarized CBP derivatives as host materials for PhOLEDs with low efficiency roll-off. Org Electron 34:237–245

53. Ghodbane A, Saffon N, Blanc S, Fery-Forgues S (2015) Influence of the halogen atom on the solid-state fluorescence properties of 2-phenyl-benzoxazole derivatives. Dyes Pigments 113:219–226
54. Gao Y, Xu W, Ma H, Obolda A, Yan W, Dong S, Zhang M, Li F (2017) Novel luminescent Benzimidazole-substituent Tris(2,4,6-trichlorophenyl)methyl radicals: Photophysics, stability, and highly efficient red-Orange electroluminescence. Chem Mater 29:6733–6739
55. Yadav AK, Pradhan B, Ulla H, Nath S, De J, Pal SK, Satyanarayan MN, Achalkumar AS (2017) Tuning the self-assembly and photophysical properties of bi-1,3,4-thiadiazole derivatives through electron donor–acceptor interactions and their application in OLEDs. J Mater Chem C 5:9345–9358
56. Sakai KI, Tsuchiya S, Kikuchi T, Akutagawa T (2016) An ESIPT fluorophore with a switchable intramolecular hydrogen bond for applications in solid-state fluorochromism and white light generation. J Mater Chem C 4:2011–2016
57. Mutai T, Tomoda H, Ohkawa T, Yabe Y, Araki K (2008) Switching of polymorph-dependent ESIPT luminescence of an Imidazo[1,2-*a*]pyridine derivative. Angew Chem Int Ed 47:9522–9524
58. Anthony SP (2011) Polymorph-dependent solid-state fluorescence and selective metal-ion-sensor properties of 2-(2-Hydroxyphenyl)-4(3*H*)-quinazolinone. Chem Asian J 7:374–379
59. Padalkar VS, Seki S (2016) Excited-state intramolecular proton-transfer (ESIPT)-inspired solid state emitters. Chem Soc Rev 45: 169–202
60. Tagare J, Ulla H, Satyanarayan MN, Vaidyanathan S (2018) Synthesis, photophysical and electroluminescence studies of new triphenylamine-phenanthroimidazole based materials for organic light emitting diodes. J Lumin 194:600–609
61. Ekbote A, Han SH, Jadhav T, Mobin SM, Lee JY, Misra R (2018) Stimuli responsive AIE active positional isomers of phenanthroimidazole as non-doped emitters in OLEDs. J Mater Chem C 6:2077–2087
62. Li Y, Xue L, Xia H, Xu B, Wen S, Tian W (2008) Synthesis and properties of polythiophene derivatives containing triphenylamine moiety and their photovoltaic applications. J Polymer Sci Part A: Polym Chem 46:3970–3984
63. Matoliukstyte A, Grazulevicius JV, Jankauskas V (2007) Glass-forming hole-transporting Triphenylamine-based Hydrazones with reactive functional groups. Mol Cryst Liq Cryst 466:85–100
64. Gao Z, Wang K, Liu F, Feng C, He X, Li J, Yang B, Zou B, Lu P (2017) Enhanced sensitivity and Piezochromic contrast through single-direction extension of molecular structure. Chem Eur J 23: 773–777
65. Szymański W, Beierle JM, Kistemaker HAV, Velema WA, Feringa BL (2013) Reversible Photocontrol of biological systems by the incorporation of molecular Photoswitches. Chem Rev 113:6114–6178
66. Raskosova A, Sto¨ßer R, Abraham W (2013) Molecular photoswitches based on spiro-acridans. Chem Commun 49: 3964–3966